

Consolidation of Vicenza, Arenaria and Istria stones: a comparison between nano-based products and acrylate derivatives

Giulia Gheno¹, Elena Badetti^{2*}, Andrea Brunelli², Renzo Ganzerla¹, Antonio Marcomini^{2*}

¹DSMN - Department of Molecular Sciences and Nanosystems, Ca' Foscari University of Venice, Scientific Campus in Via Torino 155, 30172 Mestre (VE), Italy

²DAIS - Dept. of Environmental Sciences, Informatics and Statistics, Ca' Foscari University of Venice, Scientific Campus in Via Torino 155, 30172 Mestre (VE), Italy

Abstract

Nano-based formulations are emerging as successful materials besides the use of conventional products for the consolidation of carbonate works of art e.g. stone, mortars or mural paintings. In this work, the physico-chemical characteristics, performances, and consolidation efficacy in terms of external appearance of commercial NanoRestore Ca(OH)₂ and NanoEstel SiO₂ dispersions were investigated and compared with two commercial acrylates derivatives, Acril 33 and Acril ME. The colloidal stability of the different consolidants was investigated by dynamic light scattering (DLS) and centrifugal separation analysis (CSA) techniques. As expected, acrylate emulsions showed a higher colloidal stability than the inorganic nanoparticle dispersions, with sedimentation velocity from 10⁻⁴ to 10⁻² μm/s. The examined consolidants were applied on three different stones, widely used in historical buildings in Venice: Vicenza, Arenaria and Istria stones, representing macro-, meso- and micro-porous materials, respectively. The absorption capacity, colour and gloss variation of the different stone materials were comparatively evaluated after the consolidants application. An accordance among porous structure of the substrates, hydrodynamic particle size and amount of consolidants absorbed was observed for nano-based formulations. The weathering resistance under natural and UVB aging conditions were also investigated for the consolidated stone samples, and recorded as changes of colour, gloss and surface morphology. NanoRestore and NanoEstel showed the best performances under the natural aging while the UVB irradiation seemed to not induce significant modification in the surface morphology of the treated stone samples.

Keywords: Stone consolidation; Nano-based products; Acrylate derivatives; Natural and simulated UVB aging; Colour and gloss variations

1. Introduction

The persistent exposure to the combined action of natural weathering and anthropogenic pollution over time can cause several damages to lime- and silica-based porous materials used in both artworks and architectural manufacturing. Air pollution, the presence of soluble salts and biodeteriogens [1–5] can induce flaking of the surface layers, powdering, formation of small blisters and loss of large area of the artefact [6,7]. In this context, one of the main challenges in conservation and restoration field is the use of compatible consolidants which can avoid deterioration without altering the main characteristics of the stone materials restored. Furthermore, the durability of the treatment and the long-term stability of the consolidated substrates should be ensured [8–15].

In the field of stone conservation, calcium hydroxide is one of the most promising products suitable for consolidating calcareous materials (e.g. stone sculptures, monuments or wall paintings) because it is converted into calcium carbonate as a result of carbonation, when exposed to atmospheric CO₂ under moist conditions. Ca(OH)₂ is generally applied as a saturated aqueous solution, however, due to its low solubility, large amount of solution is needed. Consequently, the treatment of stone materials with large amounts of water could be detrimental to porous matrices, favouring the pore collapse through freeze–thaw cycles and the transport of soluble salts [16]. Additional drawbacks are

51 the incomplete conversion of calcium hydroxide into calcium carbonate, as well as the post treatment
52 chromatic alteration and the low penetration depth [17]. Moreover, the stability of aqueous $\text{Ca}(\text{OH})_2$ -
53 based dispersion is not always ensured, although few exceptions are reported in literature [18]. Fast
54 clustering and sedimentation of the hydroxide particles can in fact occur, with scarce penetration and
55 veiling of the treated surface [19].

56 To enhance the consolidant performances of $\text{Ca}(\text{OH})_2$, engineered nanomaterials (ENM) based
57 formulations have been developed [20]. In detail, dispersions of $\text{Ca}(\text{OH})_2$ nanoparticles (NPs) in
58 water or short-chain alcohols have been largely studied to establish their potential use for
59 consolidation of limestone and carbonatic painted surfaces [16,21–23], wood [24], paper and canvas
60 deacidification [25], as well as for archaeological bones treatment [26]. The nano-size of the particles
61 eases the penetration of the product through porous substrates and increases the particle reactivity
62 with respect to CO_2 . Several methodologies of $\text{Ca}(\text{OH})_2$ NPs synthesis have been reported [27–32],
63 and the related formulations showed different features like degree of dispersibility, particle size
64 distribution and particle structure, which are expected to affect the consolidation process. Literature
65 studies showed that $\text{Ca}(\text{OH})_2$ NPs dispersed in short-chain alcohols exhibited a higher colloidal
66 stability than using water as dispersant, significantly improving the degree of consolidation by
67 decreasing agglomeration rate of particles [21,33,34].

68 As far as silica-based stones consolidation, commercial products containing alkoxysilanes, such as
69 tetraethoxysilane (TEOS), are commonly used [35]. These products, polymerizing in situ via a sol-
70 gel process within the porous structure of the stone to be consolidated, increase the mechanical
71 properties of the materials. However, they can form a dense microporous network of gel that tend to
72 become brittle and susceptible to cracking. Moreover, this network can obstruct the porous of the
73 materials promoting a significant reduction of water permeability [36]. To improve consolidation
74 performances, nanosilica-based products were synthesized by a template synthesis in which a
75 surfactant was used as structure-directing agent during the polymerization process. Following this
76 procedure, silica nanoparticles with uniform size and ordered mesopores were obtained. The presence
77 of surfactants avoids the cracking of the gel during the drying phase because of a coarsening of the
78 gel network that reduces the capillary pressure [37,38]. Furthermore, the advantage of using
79 nanosilica-based product with respect to the traditional solvent-based TEOS is the non-hazardous
80 solvents employed and the reduced time necessary to obtain the gel network. On the other hand, the
81 capability of silica nanoparticles to penetrate porous materials with respect to the solvent-based silica
82 product have not been yet deeply investigated [39].

83 Acrylic resins have also been largely used in conservation practice. They are thermoplastics
84 copolymers based on monomers derived from acrylic and methacrylic acid. Depending on the ratio
85 of the monomers, it is possible to structure a resin with specific molecular weight and physico-
86 chemical characteristics [40]. During the early 1930s, acrylic polymers started to be used as picture
87 varnishes because of their initial resistance to yellowing, their solubility in hydrocarbons solvents,
88 their ability to form flexible and transparent films and their glass transition temperature, preventing
89 the dirty pick-up. Unfortunately, these resins resulted unsuitable for long-term uses, due to the
90 unexpected cross-linking, cracking and yellowing exhibited when the polymers were exposed to
91 natural light [41]. At the end of the 1940s, a more stable acrylic resin system was introduced with the
92 commercial name of Paraloid. This acrylic polymer applied in solution was recommended for a wide
93 range of applications, such as textile, wood and pigments consolidants, as adhesives for paper and,
94 due to its hydrophobicity, as consolidant and water repellent for stones [42]. In particular, Paraloid
95 B72, a co-polymers of methyl methacrylate and ethyl acrylate (P(MMA/EA)) soluble in organic
96 solvents, showed an improved stability at different aging conditions [43,44]. In the last years, the
97 growing attention towards human health and environment has led to water-based emulsions safer than
98 the original formulations.

99 In this context, four different stone consolidants NanoRestore, NanoEstel, acrylic-based emulsion
100 Acril 33, and micro emulsion Acril ME were investigated. The physico-chemical characterization of
101 the commercial suspensions was performed by means of Dynamic Light scattering (DLS) and

102 Centrifugal Separation Analysis (CSA). The consolidants were then applied on three different stones,
103 i.e. Vicenza, Arenaria and Istria stone, that are representative of macro-, meso- and micro-porous
104 materials. These stones have been selected for their abundance in architectural decorative apparatus
105 of numerous venetian palaces and churches such as the Basilica of San Marco and Palazzo Ducale
106 [45]. Before the application step, Brunauer-Emmet-Teller (BET) analysis was carried out to evaluate
107 the specific surface area and the total pore volumes of the three different stone materials. Afterwards,
108 the consolidated stones samples were investigated under natural aging and laboratory test conditions,
109 i.e. UVB aging. Stereomicroscopic measurements were carried out to observe the variations in the
110 physical and morphological characteristics of the treated surfaces, while colorimetric and gloss [46]
111 measurements were performed to evaluate the chromatic variations which can occur on the surfaces
112 after the consolidation treatments due to natural and artificial aging.

114 2. Experimental section

116 2.1 Materials

117 All the commercial products tested were provided by CTS (Altavilla Vicentina, Italy). NanoRestore
118 is a 2-propanol dispersion of $\text{Ca}(\text{OH})_2$ NPs (5 g/L solid concentration). NanoEstel is an aqueous
119 colloidal dispersion of nano-sized silica (solid content 30%) stabilized with sodium hydroxide (NaOH
120 < 0.5%). Acril 33 is an aqueous emulsion (solid content 46%) of ethylacrylate and
121 methylmethacrylate co-polymer while Acril ME is a water based micro emulsion (solid content 41%)
122 of the polymer poly(butyl methacrylate).

123 Vicenza, Arenaria and Istria stones $5 \times 5 \times 2 \text{ cm}^3$ were provided by Laboratorio Morseletto (Vicenza,
124 Italy). Vicenza stone is a light ivory calcareous rock, principally composed by calcite and dolomite,
125 extracted from the Oligocene horizons in Colli Berici (Vicenza, Italy). It is the result of the
126 sedimentation of innumerable minute fossils, which create its texture, and it is usually used for stone
127 sculptures. Arenaria is a clastic sedimentary rock composed mainly by sand-sized minerals or rock
128 grains with a dark grey colour while Istria stone is a sedimentary compact rock with a micritic
129 structure and a whitish colour, formed during the lower Cretaceous. All the stones type used in this
130 study have been extensively used as building materials in venetian architectures.

132 2.2. Nano-based and acrylates consolidants characterization

133 The dispersion stability of each consolidant was carried out by Dynamic Light scattering (DLS) and
134 Centrifugal Separation Analysis (CSA). Hydrodynamic particle diameter was measured by DLS by
135 means of a multi-angle Nicomp ZLS Z3000 (Particle Sizing System, Port Richey, FL, USA) with an
136 optical fiber set at 90° scattering angle ($W=25 \text{ mW}$, $\lambda=639 \text{ nm}$, at 25°C). Particle sedimentation
137 velocity was calculated by CSA, employing the Multiwavelength Dispersion Analyzer LUMiSizer
138 651 at $\lambda=470 \text{ nm}$. Briefly, the samples were analysed in polycarbonate cuvette with 10 mm optical
139 path every 50 seconds at 25°C and 2800 Rotation Per Minute (RPM). The transmission profiles,
140 which are the raw data generated by CSA, moved from the lowest values of transmittance (indicating
141 the highest amount of particles in the suspension) to the maximum transmittance, corresponding to
142 the total sedimentation of particles in the cuvette (i.e. plateau). The variation of the transmission
143 profiles over time and space allowed to calculate particle sedimentation velocity [47]. The overall
144 results from DLS and CSA were reported as an average of three independent measurements.

145 After the physico-chemical characterization of the commercial dispersions, the consolidation test was
146 carried out by applying Nanorestore, NanoEstel, Acril 33 and Acril ME on Vicenza, Arenaria and
147 Istria stones. Before the consolidation treatment, the stone blocks were carefully washed and brushed
148 in distilled water for 3 times in order to remove all the soluble salts and then dried in a static oven at
149 60°C . The consolidants were applied by brush until refusal and the samples were maintained in
150 controlled conditions ($T=25^\circ\text{C}$ and $UR=30\%$) until reaching a constant weight. The amount of
151 absorbed product was estimate as the difference in weight between the consolidated and the untreated

152 stone samples for three independent measurements (10 weight measurements for each consolidated
153 stone). Three samples for each substrate were prepared.

154

155 2.3. *Stones characterization*

156 Stereomicroscopic measurements were carried out with a Nikon SMZ1270 with magnifications of 10
157 or 20x on the treated surfaces. The films morphology was recorded by a Nikon DS-Fi2 camera with
158 Nikon Digital Sight DS-L3 software.

159 Brunauer-Emmet-Teller (BET) analysis was carried out using a ASAP 2010 of MicroMetrics to
160 evaluate the specific surface area ($\text{m}^2 \text{g}^{-1}$) and the total pore volumes of the different stones using
161 nitrogen multilayer adsorption measured as a function of relative pressure. Before BET analysis the
162 samples were degassed at 10^{-3} Torr at 130°C for 12 hours. BET analysis was conducted at -196°C ,
163 temperature of condensation of the N_2 . The total pores volume was determined at P/P_0 of 0.98.

164 The stones consolidated with the tested formulations were investigated as fresh and under natural and
165 UVB aging conditions. Natural aging of the samples was carried out exposing the samples to Venice-
166 Mestre (Italy) outdoor conditions in a rigid plastic support with an inclination of 60° over 2 years.
167 UV accelerated aging tests were carried out in a UVB chamber, under a monochromatic UVB
168 radiation ($\lambda=254 \text{ nm}$) at $28 \pm 2^\circ\text{C}$ and relative humidity of 45% up to 1200 hours. The variation of
169 treated samples color was monitored at incremental time intervals, monthly for natural aging and 100
170 hours for the UVB aging. The colour measurements were carried out by a Konica Minolta
171 spectrophotometer according to CIE Lab colour space method [48,49]. The parameters L^* , a^* , b^*
172 were simultaneously collected. L^* stands for the lightness ($L^*=0$ corresponds to black, $L^*=100$
173 corresponds to white), while a^* and b^* are the colour-opponent dimensions: a^* is the red/green
174 balance ($-a^*$ corresponds to green and $+a^*$ corresponds to red) and b^* is the yellow/blue balance ($-b^*$
175 corresponds to blue and $+b^*$ corresponds to yellow). The total variation of colour (ΔE^*) was
176 calculated by the equation $[(\Delta L^*)^2 + (\Delta a^*)^2 + (\Delta b^*)^2]^{1/2}$. The parameters ΔL^* , Δa^* and Δb^* refer to the
177 difference between the aged samples and the untreated ones ($\Delta L^* = L^*_{t=x} - L^*_{t=0}$; $\Delta a^* = a^*_{t=x} - a^*_{t=0}$;
178 $\Delta b^* = b^*_{t=x} - b^*_{t=0}$).

179 The specular gloss of the untreated, treated and aged stone samples, i.e. the ratio of the luminous flux
180 reflected from the samples in the specular direction for a specified source and receptor angle, was
181 determined with a Picogloss 503 (Erichsen) at the incident angle of 20° with a resolution of 1 GU,
182 according to ASTM D523-08, 2004 [28]. The gloss retention ($\Delta\text{gloss} \%$) was calculated between the
183 untreated and the consolidated surface as $[(\text{gloss}_{(\text{untreated})} - \text{gloss}_{(\text{treated})}) / \text{gloss}_{(\text{untreated})} \times 100]$ and
184 between the unaged and aged samples as $[(\text{gloss}_{(t=0)} - \text{gloss}_{(t=x)}) / \text{gloss}_{(t=0)} \times 100]$.

185

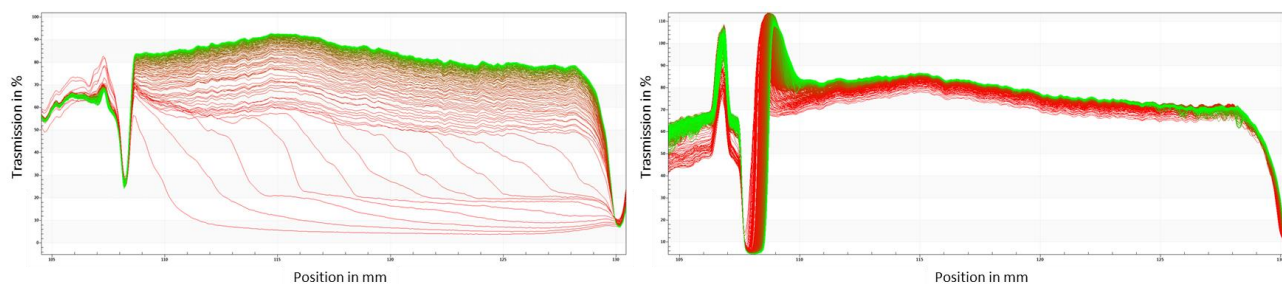
186 3. Results and discussion

187

188 3.1. *Colloidal characterization of consolidants*

189 The colloidal stability of Nanorestore $\text{Ca}(\text{OH})_2$ and NanoEstel SiO_2 NPs dispersions was investigated
190 by CSA and DLS techniques. In detail, as far as particle sedimentation velocity, a method already
191 developed [50] was applied to Nanorestore and Nanoestel, and the transmittance profiles of the two
192 nano-based dispersions are displayed in Figure 1. As it can be clearly observed by transmittance
193 profiles, the settling of Nanoestel NPs is very low if compared to Nanorestore results, showing
194 sedimentation velocities $\leq 0.01 \mu\text{m/s}$ at gravity vs $0.04 \mu\text{m/s}$ calculated for Nanorestore. This
195 indicates the higher stability of Nanoestel with respect to Nanorestore in alcoholic dispersion.

196



197

198

199

200

201

202

203

204

205

206

207

208

209

210

211

212

213

214

215

216

217

218

219

220

221

222

223

224

225

226

227

Figure 1 – Typical transmission profiles at 2800 RPM of Nanorestore dispersion (left) and Nanoestel dispersion (right).

Furthermore, hydrodynamic particle size of the tested dispersions was determined by DLS. A population with an average hydrodynamic particle size of 336 ± 34 nm was detected for Nanorestore dispersion while 165 ± 28 nm was obtained for Nanoestel.

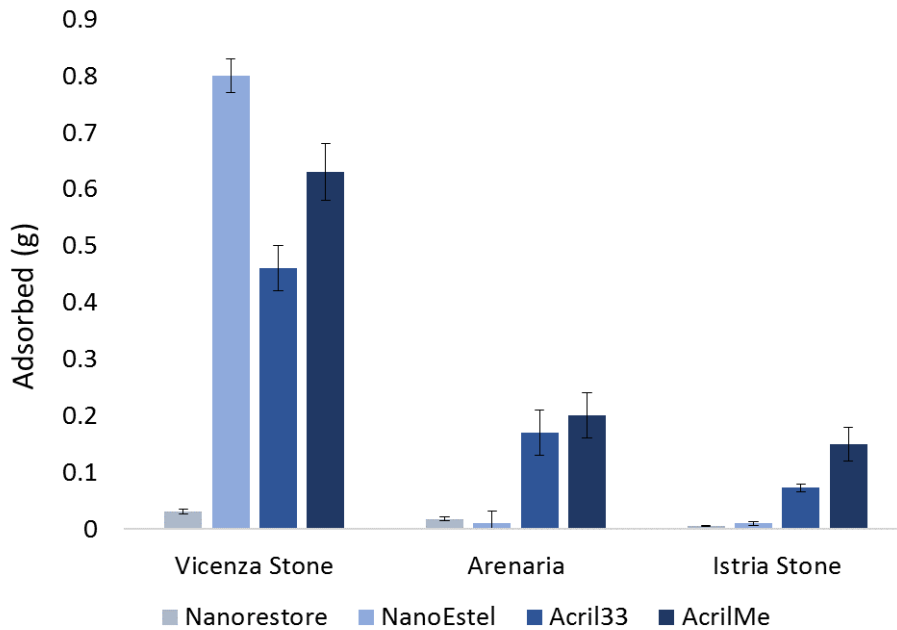
As far as the acrylic derivatives, the emulsions were opportunely diluted for CSA and DLS measurements (see Figure S1 in the Supporting Information). Sedimentation velocity values and average size distribution were $\leq 3 \times 10^{-4}$ $\mu\text{m/s}$ and 70 ± 15 nm for Acril 33 and $\leq 8 \times 10^{-4}$ $\mu\text{m/s}$ and 47 ± 7 nm for Acril ME. In conclusion, the highest colloidal stability of both acrylic emulsions with respect to the nano-based dispersions investigated was proved.

3.2. Stone surface characterization

3.2.1. Consolidated stones

The surface area and the total pore volumes of the different stones were investigated by BET method before the consolidants applications, and confirmed the micro- meso- and macro-porosity of Istria, Arenaria and Vicenza stone respectively (Table S1 in SI).

The amount of Nanorestore, Nanoestel, Acril 33 and Acril ME adsorbed on the three different stone substrates was measured as weight difference and the overall data are reported in SI (Table S2). Adsorption results (Figure 2), according to BET measurements, showed as Vicenza stone is the material with the highest capacity to adsorb the consolidants investigated because of its biggest pores size. On the other hand, Istria stone showed the lowest adsorption of consolidants, as expected for a micro-porous material. Comparing the recorded amounts of the different consolidants adsorbed, Nanorestore and Nanoestel showed the lowest values of adsorption (< 0.04 g) for each stone investigated, except for Nanoestel which was strongly adsorbed on Vicenza stone (0.80 g). Acril 33 and Acril Me were instead absorbed in relevant amounts with respect to inorganic nano-based materials by all the stones investigated. This finding can be ascribed to the different way in which inorganic NPs and acrylates interact with the substrates, acrylates in fact usually form a film on the surface of the stones.

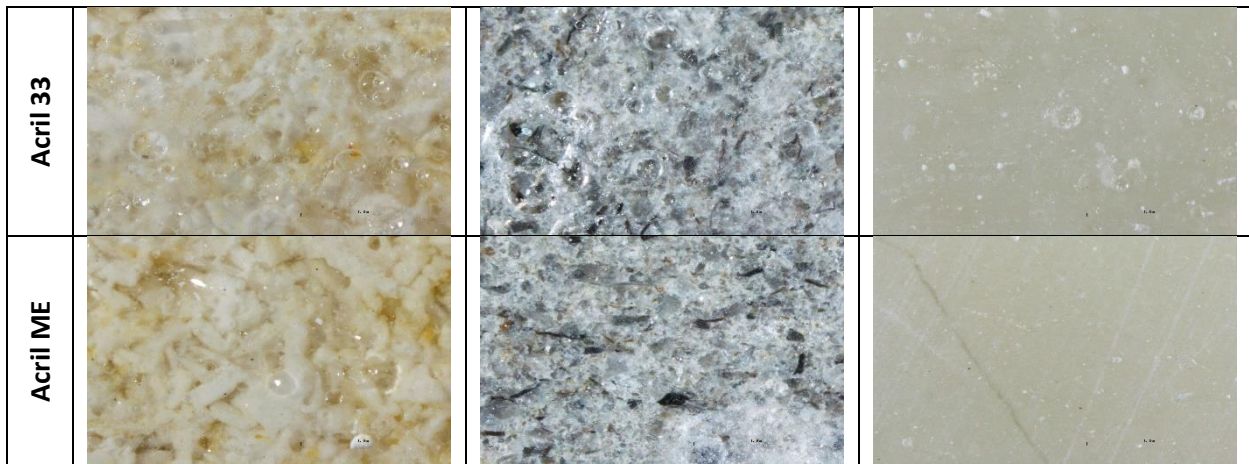


228
 229 Figure 2. Comparison among NanoRestore, NanoEstel, Acril 33 and Acril ME adsorption from
 230 Vicenza, Arenaria and Istria stones.

231
 232 To better understand this behaviour, the surface morphology of Vicenza, Arenaria and Istria stones
 233 was further investigated by Stereo Microscope analysis (Figure 3), before and after each consolidation
 234 treatment. The results highlighted that the stone samples treated with NanoRestore underwent a
 235 slightly whitened of the surface. As far as the surface treated with NanoEstel, a thin homogenous
 236 transparent and bright film without cracks was observed, while Acril 33 and Acril ME completely
 237 changed the original aspects of the stone supports creating a transparent, bright and thick film with a
 238 large number of air bubbles. In result, the polymeric layer covering the surface appeared to change
 239 the natural morphology of the stone and to occlude the pores.

240

	Vicenza stone	Arenaria	Istria stone
Untreated			
NanoRestore			
NanoEstel			



241
242 Figure 3. Micrographs (20x) of the surface morphology of the stone samples before (untreated) and
243 after the consolidation treatment with NanoRestore, NanoEstel, Acril 33 and Acril ME.
244

245 Furthermore, colorimetric and gloss analysis allowed to observe variations in terms of ΔE and $\Delta gloss$
246 % with respect to the untreated stones (Table 1). A general tendency of the treated stone samples to
247 yellowing was observed and, as it can be seen in the color graph of Figure 4, this chromatic variation
248 induced the simultaneous decrease of a^* values (shift to green shades) and the increase of b^* values
249 (shift to yellowing shades). On the other hand, the lightness variations (i.e. increment in the L^*
250 values), as shown in Table 1 indicated a slightly shift towards clearer shades (whitening effect of the
251 consolidants). This behavior was shown mostly for the stone samples consolidates with $Ca(OH)_2$ NPs.
252 In general, the overall results in Table 1 for Vicenza stone highlighted the best performances of
253 NanoRestore in terms of colour and gloss retention among the consolidants tested, showing the lowest
254 ΔE (7.96) and $\Delta gloss$ % (-13) values. Small colour and gloss variations ($\Delta E= 8.78$ and $\Delta gloss$ %=
255 33) were also recorded after NanoEstel treatment. Thus, both the inorganic NPs exhibited good
256 consolidant performances by maintaining the original characteristics of the untreated surface.
257 However, they presented opposite trends in term of gloss variation. NanoRestore in fact, induced a
258 slightly decrease in the gloss of the treated surface (negative values of $\Delta gloss$ %, indicating an
259 increase of the surface brilliance), while NanoEstel showed positive values of $\Delta gloss$ % (indicating
260 more opacity than the untreated material). On the other hand, significant variations of colour and
261 gloss retention were recorded for Vicenza stone treated with the two acrylic-based consolidants. In
262 particular, the highest values of $\Delta gloss$ % (-173) recorded for Vicenza stone treated with Acril 33,
263 highlighted a surface modification after the treatment.

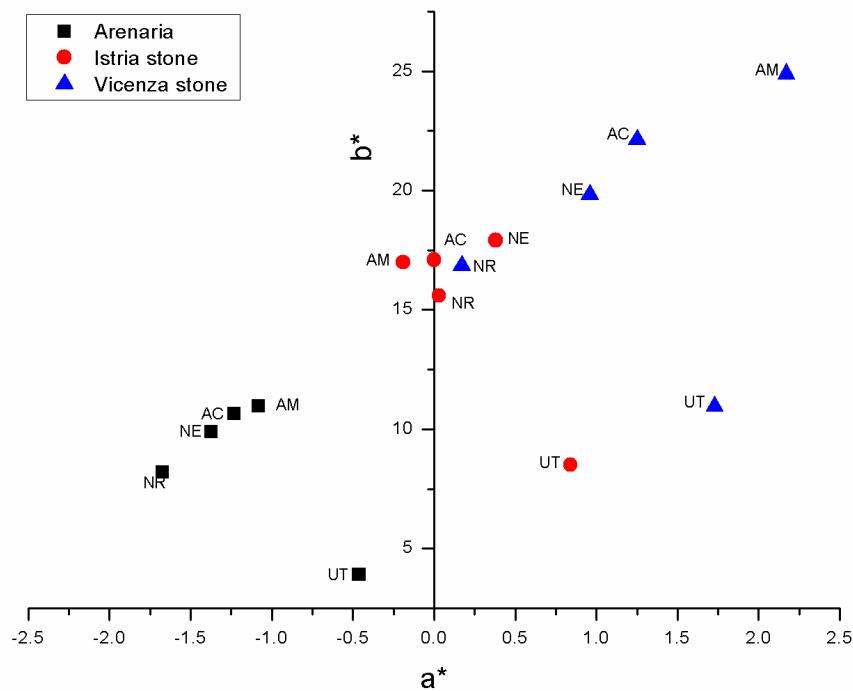
264 As far as Arenaria, even if Acril 33 and Acril ME seemed the most compatible consolidants with ΔE
265 values of 6.67 and 6.63 respectively, they formed a glossy layer on the surface of the stones that
266 changes significantly the gloss values of the original materials with extremely high $\Delta gloss$ %
267 variations in both cases.

268 Finally, taking into account Istria stone, the most compatible consolidant was also in this case
269 NanoRestore (Table 1), which induced a slightly whitening of the surface but not a significant
270 variation in the colour parameters ($\Delta E=7.57$) and in the gloss values ($\Delta gloss$ %=-18). The nanosilica-
271 based consolidant induces similar variation in the colour parameters ($\Delta E = 9.44$) but higher gloss
272 variations ($\Delta gloss$ %=-51) with respect to Nanorestore. Acrylates present high gloss variations of the
273 treated surfaces towards highly negative values, indicating an increase of the surface brilliance after
274 the stone treatment. In conclusion, the overall results in Table 1 suggested that the inorganic NPs
275 consolidants showed the lowest colour and gloss surface variation for all the treated stones.
276

277 Table 1. Colour parameters Δa^* , Δb^* , ΔL^* and ΔE and gloss variation ($\Delta gloss\%$) values determined
 278 for Vicenza, Arenaria and Istria stone after the consolidation treatments with NanoRestore,
 279 NanoEstel, Acril 33 and Acril ME.

Stone sample	Consolidant	Δa^*	Δb^*	ΔL^*	ΔE	$\Delta gloss\%$
Vicenza	NanoRestore	-1.59	5.89	5.11	7.96	-13
	NanoEstel	-0.97	8.17	3.08	8.78	33
	Acril 33	-0.62	11.25	1.90	11.42	-173
	Acril ME	0.30	13.58	-1.94	13.72	-39
Arenaria	NanoRestore	-1.10	5.46	5.43	7.78	-22
	NanoEstel	-0.83	7.11	0.29	7.16	-54
	Acril 33	-0.82	6.56	0.88	6.67	-1109
	Acril ME	-0.70	6.59	0.11	6.63	-1256
Istria	NanoRestore	-0.74	6.64	3.55	7.57	-18
	NanoEstel	-0.58	9.15	2.25	9.44	-51
	Acril 33	-0.85	8.56	2.24	8.89	-666
	Acril ME	-1.16	8.39	0.85	8.51	-527

280
281



282
 283 Figure 4. Plot of a^* vs b^* values (color graph) determined for untreated (UT) Vicenza stone (Δ),
 284 Arenaria (\square) and Istria stone (O) and treated samples with NanoRestore (NR), NanoEstel (NE), Acril
 285 33 (AC) and Acril ME (AM).
 286

287 3.2.2. Natural and UVB aging of treated stones

288 Stone samples treated with NanoRestore, NanoEstel, Acril 33 and Acril ME were exposed to different
 289 aging environments, a natural outdoor aging over 2 years (in Venice-Mestre, Italy), and an artificial
 290 (UVB) aging for 1200 hours. Total color (ΔE) and gloss ($\Delta gloss\%$) variations values obtained after
 291 both aging experiments are reported in Table 2.
 292

293 Table 2. ΔE and $\Delta gloss\%$ values determined for Vicenza, Arenaria and Istria stone after natural
 294 outdoor and UVB aging.

Stone sample	Consolidant	Natural aging		UVB aging	
		ΔE	$\Delta gloss \%$	ΔE	$\Delta gloss \%$
Vicenza	NanoRestore	24.21	61	3.94	-8
	NanoEstel	21.63	50	2.98	-25
	Acril 33	25.61	59	4.88	-37
	Acril ME	24.18	75	4.18	-75
Arenaria	NanoRestore	9.90	33	1.51	-16
	NanoEstel	8.88	25	1.84	-37
	Acril 33	17.59	97	3.15	-17
	Acril ME	24.85	97	2.79	-24
Istria	NanoRestore	9.78	44	3.73	-22
	NanoEstel	11.43	40	2.67	-7
	Acril 33	22.43	91	2.85	-34
	Acril ME	18.39	87	3.85	-57

295

296

297

298

299

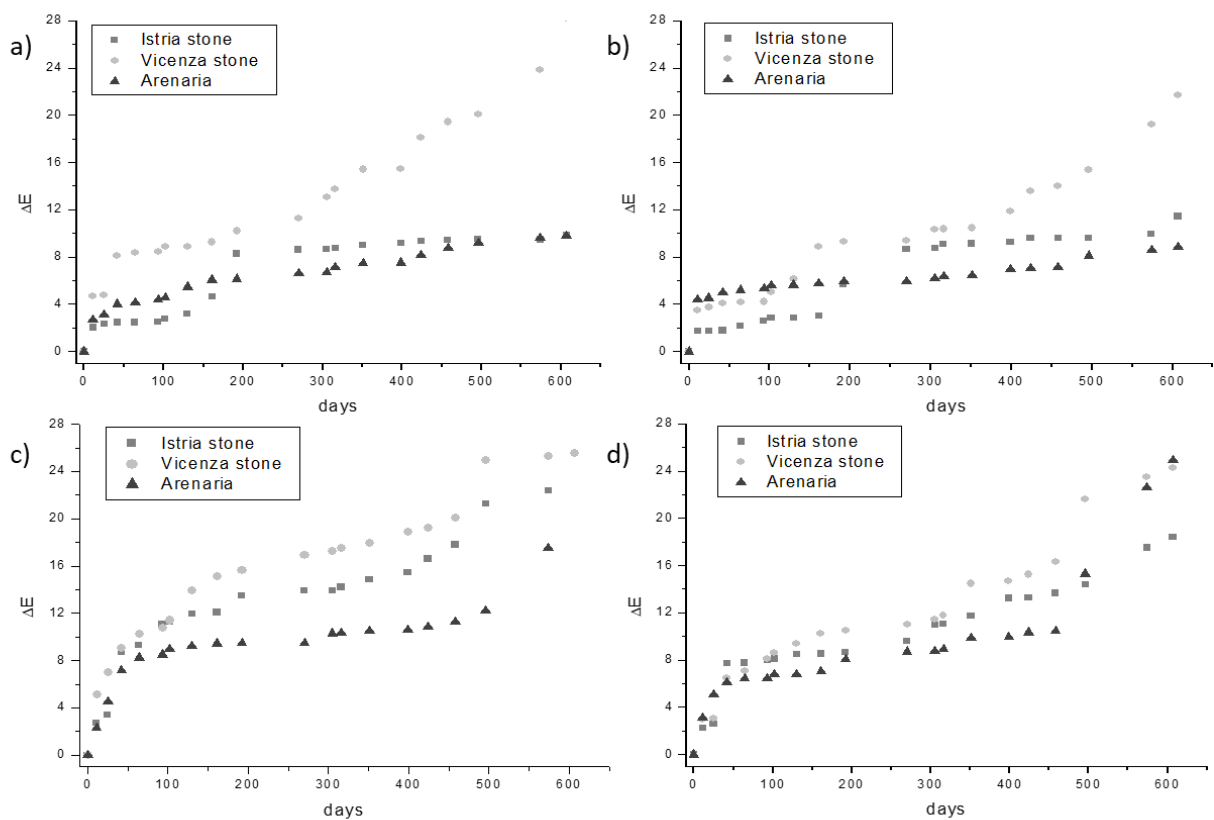
300

301

302

303

As far as natural aging, Vicenza stone treated samples showed the highest ΔE variations regardless the consolidant applied, with values ranging from 21.6 to 25.6, while for Arenaria and Istria stones, the lowest ΔE values were observed for samples treated with nano-based consolidants (values ten times lower than those obtained for the treatment with acrylate derivatives). Furthermore, ΔE variations over time were also investigated along the two years of aging experiments performed, and the overall results obtained for each consolidant are reported in Figure 5. From these data it can be clearly observed the highest and fast increment of ΔE for all the stones samples treated with Acril 33 and Acril Me emulsions.



304

305

306

307

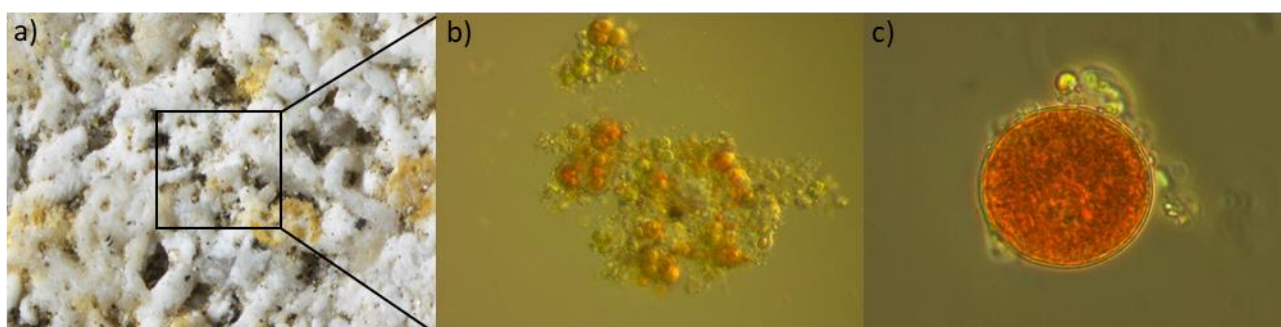
308

Figure 5 – ΔE parameter determined for the samples of Vicenza, Arenaria and Istria stone treated with (a) NanoRestore, (b) NanoEstel, (c) Acril 33 and (d) Acril ME and exposed at incremental time of natural outdoor aging conditions.

309 In detail, as displayed by the color graph reported in Figure S2 (SI), the total chromatic variations
310 observed for the different stones are principally linked to a shift in the coordination color towards a
311 red-brown dye. Moreover, as reported in Figure S3 and Figure S4 (SI), a decrease of L^* values was
312 recorded for Vicenza and Arenaria stones treated with the different consolidants, except for Arenaria
313 with NanoEstel. In this last case, a whitening of the surface occurred, probably due to the formation
314 of a thick silica-based layer derived from the crosslinking of the consolidants precursor. On the other
315 hand, as showed in Figure S5 (SI), no significant variation in terms of lightness was determined for
316 Istria stone exposed to natural aging, except for the samples treated with the two acrylic-based
317 products, highlighting a massive darkening of the surface.

318 The colorimetric changes observed were mainly ascribed to deposition and entrapment of dust and
319 atmospheric particles into the stone pores, as shown in Figure S6 (SI). In the specific case of aged
320 Vicenza stone samples, the shift towards the dark red colour observed (Figure S2 in SI) was finally
321 attributed to the presence and diffuse growth of freshwater *Chlorophyta* microalgae, from the family
322 of *Haematococcaceae*. Optical microscope analysis (Figure 6) highlighted the presence of this
323 unicellular microalgae (size ranging from 40 to 120 μm), which contains blood-red carotenoid
324 pigment astaxanthin (3,3'-dihydroxy- β,β -carotene-4,4'-dione) in the cytoplasmic lipid globules of
325 their cells. These pigments are produced and rapidly accumulated when the environmental conditions
326 become unfavourable for normal cell growth [51,52], explaining the dark red colour observed in
327 treated Vicenza stones after the natural aging process.

328



329

330

331 Figure 6- Micrographs of Vicenza stone treated with NanoRestore and exposed over two years to
332 outdoor conditions. a) stone surface at 20x; b) *Chlorophyta* microalgae observed on the surface at
333 200x, c) *Chlorophyta* microalgae at 400x.

334

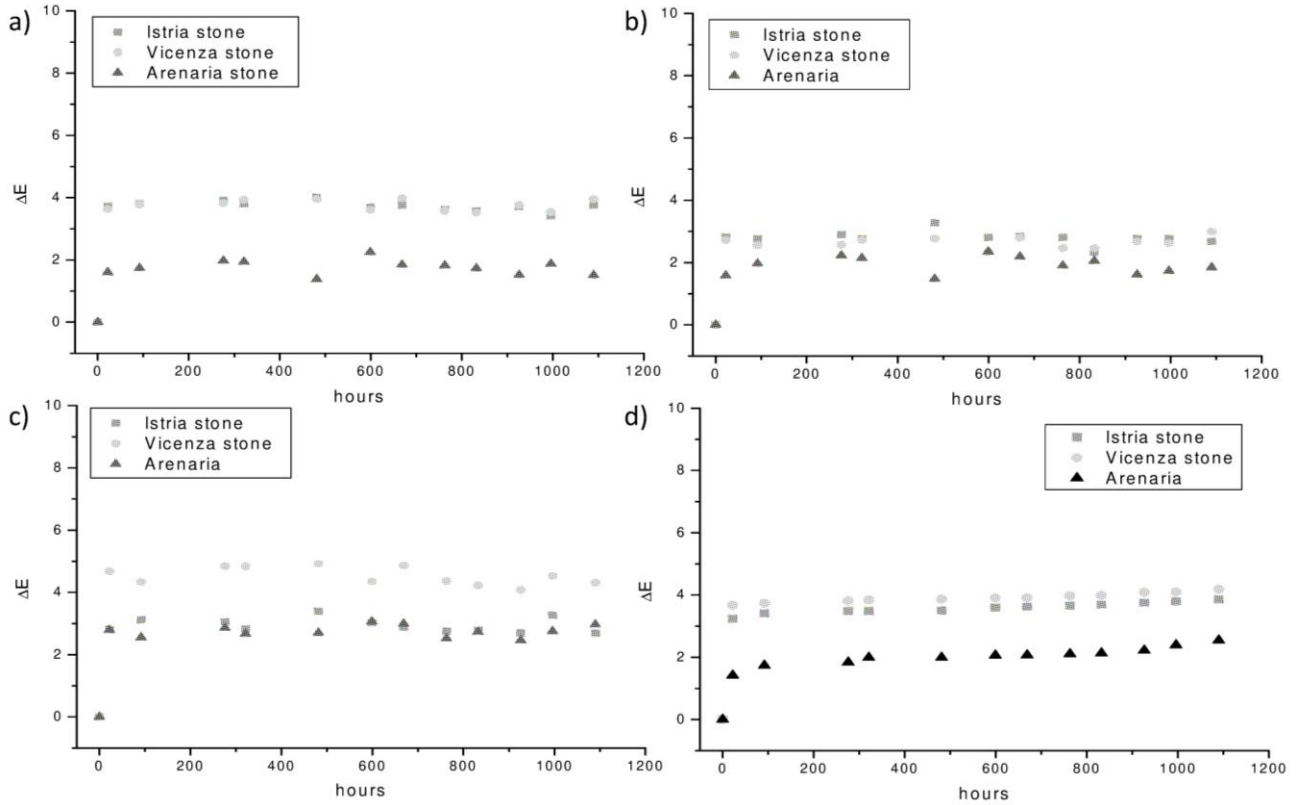
335 Concerning $\Delta\text{gloss \%}$ (Table 2), the natural aging induced a reduction in the gloss values for all the
336 stone samples investigated ($\Delta\text{gloss \%} > 0$). This indicate an opacification of the surface layers treated
337 with the different consolidants. In detail, the inorganic NPs products, NanoRestore and NanoEstel,
338 showed low gloss variations always $< 50\%$ for all the treated materials except for Vicenza stone
339 treated with Nanorestore (61%). The best performances for these consolidants were obtained in the
340 treatment of Arenaria. On the other hand, Acril 33 and Acril ME consolidants induced a highest
341 opacification of the treated surfaces with $\Delta\text{gloss \%}$ ranging from 59 to 97%.

342 As far as UVB aging (Table 2), the laboratory conditions employed for the test seemed to not induce
343 any significant color variation of the treated stone surfaces, showing ΔE always < 5 . Also in this case,
344 ΔE variations over time were investigated (Figure 7), confirming the low color alteration induced by
345 UVB aging conditions over 1200 hours of analysis.

346 Moreover, according to the stereo microscope images (Figure S7 in SI), the surface appeared to be
347 similar to the one of the original untreated stones, and the formation of craquelure or microfractures
348 was not observed after 1200 hours of UVB aging.

349 As far as $\Delta\text{gloss \%}$ (Table 2), conversely to what observed during natural aging, UVB aging induced
350 an increase in the gloss values of the surface. The increment of the brightness of the surface can be
351 explained, in the cases of polymeric consolidants film of NanoEstel, Acril 33 and Acril Me, with an

352 increase of the degree of polymerization of the commercial products exposed to UVB irradiation [53].
 353 Furthermore, in the case of the NanoRestore, the increment of gloss can be ascribed to a further
 354 conversion of $\text{Ca}(\text{OH})_2$ NPs to CaCO_3 [18]. In general, a good resistance to photo-degradation was
 355 observed for all the stone surfaces treated with both the inorganic consolidants and Acril33, with
 356 $\Delta\text{gloss } \%$ values ranging from -37 to -7, while high variations were observed for AcrilMe (up to -75).
 357



358
 359 Figure 7 – ΔE parameter determined for the samples of Vicenza, Arenaria and Istria stone treated
 360 with (a) NanoRestore, (b) NanoEstel, (c) Acril 33 and (d) Acril ME and exposed at incremental time
 361 of UVB aging conditions.
 362

363 4. Conclusions

364
 365 In this study, commercial Nanorestore, Nanoestel, Acril 33 and Acril ME were applied on Vicenza,
 366 Arenaria and Istria stones, for investigating their surface appearance after the consolidation treatment.
 367 The overall results obtained by the followed approach, in which colorimetric and gloss measurements
 368 were combined with stereo microscope analysis and adsorption measurements, provided useful
 369 insights on the most suitable product in the stones consolidation with respect to Venice environment.
 370 In detail, the worst performances in terms of highest colour and gloss alterations of the stones surface
 371 were observed under natural aging conditions with respect to UVB. Among the three stones
 372 investigated, Vicenza stone resulted the most sensitive material towards aging degradation after the
 373 treatment with all the consolidants, while among all the consolidants applied, nano-based materials
 374 showed the best performances, highlighting the importance of nanotechnology in stone conservation
 375 field.
 376

377 **Conflict of interest statement**

378

379 We declare that we have no financial and personal relationships with other people or organizations
380 that can inappropriately influence our work, there is no professional or other personal interest of any
381 nature or kind in any product, service or company that could be construed as influencing the position
382 presented in, or the review of, the manuscript entitled.

383

384 **Acknowledgements**

385

386 The authors are grateful to University Ca' Foscari of Venice for the financial support and to C.T.S.
387 S.p.A. (Altavilla Vicentina, Vicenza, Italy) for the consolidants products investigated.

388

389

390 **References**

- 391
- 392 [1] F. Corvo, J. Reyes, C. Valdes, F. Villaseñor, O. Cuesta, D. Aguilar, P. Quintana, Influence of
393 Air Pollution and Humidity on Limestone Materials Degradation in Historical Buildings
394 Located in Cities Under Tropical Coastal Climates, *Water. Air. Soil Pollut.* 205 (2009) 359.
395 doi:10.1007/s11270-009-0081-1.
- 396 [2] A.H. Webb, R.J. Bawden, A.K. Busby, J.N. Hopkins, Studies on the effects of air pollution on
397 limestone degradation in Great Britain, *Atmos. Environ. Part B. Urban Atmos.* 26 (1992) 165–
398 181. doi:https://doi.org/10.1016/0957-1272(92)90020-S.
- 399 [3] M. Maguregui, A. Sarmiento, I. Martínez-Arkarazo, M. Angulo, K. Castro, G. Arana, N.
400 Etxebarria, J.M. Madariaga, Analytical diagnosis methodology to evaluate nitrate impact on
401 historical building materials, *Anal. Bioanal. Chem.* 391 (2008) 1361–1370.
402 doi:10.1007/s00216-008-1844-z.
- 403 [4] M.F. Orihuela, J. Abad, J.F. González Martínez, F.J. Fernández, J. Colchero, Nanoscale
404 characterisation of limestone degradation using Scanning Force Microscopy and its correlation
405 to optical appearance, *Eng. Geol.* 179 (2014) 158–166.
406 doi:https://doi.org/10.1016/j.enggeo.2014.06.022.
- 407 [5] G. Caneva, M.P. Nugari, O. Salvadori, *La biologia vegetale per i beni culturali*, Vol I, 2nd ed.,
408 2007.
- 409 [6] L. Toniolo, M. Boriani, G. Guidi, *Built Heritage: Monitoring Conservation Management*,
410 Switzerland, 2015.
- 411 [7] S.Y. Xie, J.F. Shao, W.Y. Xu, Influences of chemical degradation on mechanical behaviour of
412 a limestone, *Int. J. Rock Mech. Min. Sci.* 48 (2011) 741–747.
413 doi:https://doi.org/10.1016/j.ijrmms.2011.04.015.
- 414 [8] M. Matteini, *Conservation Science in Cultural Heritage - Vol. 8*, 2008.
- 415 [9] C. Conti, C. Colombo, D. Dellasega, M. Matteini, M. Realini, G. Zerbi, Ammonium oxalate
416 treatment: Evaluation by μ -Raman mapping of the penetration depth in different plasters, *J.*
417 *Cult. Herit.* 12 (2011) 372–379. doi:https://doi.org/10.1016/j.culher.2011.03.004.
- 418 [10] B. Doherty, M. Pamplona, R. Selvaggi, C. Miliani, M. Matteini, A. Sgamellotti, B. Brunetti,
419 Efficiency and resistance of the artificial oxalate protection treatment on marble against
420 chemical weathering, *Appl. Surf. Sci.* 253 (2007) 4477–4484.
421 doi:https://doi.org/10.1016/j.apsusc.2006.09.056.
- 422 [11] C. Conti, I. Aliatis, M. Casati, C. Colombo, M. Matteini, R. Negrotti, M. Realini, G. Zerbi,
423 Diethyl oxalate as a new potential conservation product for decayed carbonatic substrates, *J.*
424 *Cult. Herit.* 15 (2014) 336–338. doi:https://doi.org/10.1016/j.culher.2013.08.002.
- 425 [12] D. Chelazzi, G. Poggi, Y. Jaidar, N. Toccafondi, R. Giorgi, P. Baglioni, Hydroxide
426 nanoparticles for cultural heritage: Consolidation and protection of wall paintings and
427 carbonate materials, *J. Colloid Interface Sci.* 392 (2013) 42–49.
428 doi:https://doi.org/10.1016/j.jcis.2012.09.069.
- 429 [13] R. Giorgi, M. Ambrosi, N. Toccafondi, P. Baglioni, Nanoparticles for Cultural Heritage
430 Conservation: Calcium and Barium Hydroxide Nanoparticles for Wall Painting Consolidation,
431 *Chem. – A Eur. J.* 16 (2010) 9374–9382. doi:10.1002/chem.201001443.

- 432 [14] R. Giorgi, L. Dei, P. Baglioni, A New Method for Consolidating Wall Paintings Based on
433 Dispersions of Lime in Alcohol, *Stud. Conserv.* 45 (2000) 154–161.
434 doi:10.1179/sic.2000.45.3.154.
- 435 [15] A. Pondelak, S. Kramar, M.L. Kikelj, A. Sever Škapin, In-situ study of the consolidation of
436 wall paintings using commercial and newly developed consolidants, *J. Cult. Herit.* 28 (2017)
437 1–8. doi:https://doi.org/10.1016/j.culher.2017.05.014.
- 438 [16] P. Baglioni, D. Chelazzi, R. Giorgi, G. Poggi, Colloid and Materials Science for the
439 Conservation of Cultural Heritage: Cleaning, Consolidation, and Deacidification, *Langmuir.*
440 29 (2013) 5110–5122. doi:10.1021/la304456n.
- 441 [17] V. Daniele, G. Taglieri, R. Quaresima, The nanolimes in Cultural Heritage conservation:
442 Characterisation and analysis of the carbonatation process, *J. Cult. Herit.* 9 (2008) 294–301.
443 doi:https://doi.org/10.1016/j.culher.2007.10.007.
- 444 [18] C. Rodriguez-Navarro, E. Ruiz-Agudo, M. Ortega-Huertas, E. Hansen, Nanostructure and
445 Irreversible Colloidal Behavior of Ca(OH)₂: Implications in Cultural Heritage Conservation,
446 *Langmuir.* 21 (2005) 10948–10957. doi:10.1021/la051338f.
- 447 [19] P. Baglioni, D. Chelazzi, R. Giorgi, E. Carretti, N. Toccafondi, Y. Jaidar, Commercial
448 Ca(OH)₂ nanoparticles for the consolidation of immovable works of art, *Appl. Phys. A.* 114
449 (2014) 723–732. doi:10.1007/s00339-013-7942-6.
- 450 [20] P. Baglioni, D. Chelazzi, Nanoscience for the Conservation of Works of Art, *The Royal*
451 *Society of Chemistry*, 2013. doi:10.1039/9781849737630.
- 452 [21] M. Ambrosi, L. Dei, R. Giorgi, C. Neto, P. Baglioni, Colloidal Particles of Ca(OH)₂:
453 Properties and Applications to Restoration of Frescoes, *Langmuir.* 17 (2001) 4251–4255.
454 doi:10.1021/la010269b.
- 455 [22] L. Dei, B. Salvadori, Nanotechnology in cultural heritage conservation: nanometric slaked
456 lime saves architectonic and artistic surfaces from decay, *J. Cult. Herit.* 7 (2006) 110–115.
457 doi:https://doi.org/10.1016/j.culher.2006.02.001.
- 458 [23] I. Natali, M.L. Saladino, F. Andriulo, D. Chillura Martino, E. Caponetti, E. Carretti, L. Dei,
459 Consolidation and protection by nanolime: Recent advances for the conservation of the graffiti,
460 Carceri dello Steri Palermo and of the 18th century lunettes, SS. Giuda e Simone Cloister,
461 Corniola (Empoli), *J. Cult. Herit.* 15 (2014) 151–158.
462 doi:https://doi.org/10.1016/j.culher.2013.03.002.
- 463 [24] R. Giorgi, D. Chelazzi, P. Baglioni, Nanoparticles of Calcium Hydroxide for Wood
464 Conservation. The Deacidification of the Vasa Warship, *Langmuir.* 21 (2005) 10743–10748.
465 doi:10.1021/la0506731.
- 466 [25] R. Giorgi, L. Dei, M. Ceccato, C. Schettino, P. Baglioni, Nanotechnologies for Conservation
467 of Cultural Heritage: Paper and Canvas Deacidification, *Langmuir.* 18 (2002) 8198–8203.
468 doi:10.1021/la025964d.
- 469 [26] I. Natali, P. Tempesti, E. Carretti, M. Potenza, S. Sansoni, P. Baglioni, L. Dei, Aragonite
470 Crystals Grown on Bones by Reaction of CO₂ with Nanostructured Ca(OH)₂ in the Presence
471 of Collagen. Implications in Archaeology and Paleontology, *Langmuir.* 30 (2014) 660–668.
472 doi:10.1021/la404085v.
- 473 [27] B. Salvadori, L. Dei, Synthesis of Ca(OH)₂ Nanoparticles from Diols, *Langmuir.* 17 (2001)

- 474 2371–2374. doi:10.1021/la0015967.
- 475 [28] A. Nanni, L. Dei, Ca(OH)₂ Nanoparticles from W/O Microemulsions, *Langmuir*. 19 (2003)
476 933–938. doi:10.1021/la026428o.
- 477 [29] T. Liu, Y. Zhu, X. Zhang, T. Zhang, T. Zhang, X. Li, Synthesis and characterization of calcium
478 hydroxide nanoparticles by hydrogen plasma-metal reaction method, *Mater. Lett.* 64 (2010)
479 2575–2577. doi:https://doi.org/10.1016/j.matlet.2010.08.050.
- 480 [30] V. Daniele, G. Taglieri, Nanolime suspensions applied on natural lithotypes: The influence of
481 concentration and residual water content on carbonation process and on treatment
482 effectiveness, *J. Cult. Herit.* 11 (2010) 102–106.
483 doi:https://doi.org/10.1016/j.culher.2009.04.001.
- 484 [31] V. Daniele, G. Taglieri, Synthesis of Ca(OH)₂ nanoparticles with the addition of Triton X-
485 100. Protective treatments on natural stones: Preliminary results, *J. Cult. Herit.* 13 (2012) 40–
486 46. doi:https://doi.org/10.1016/j.culher.2011.05.007.
- 487 [32] E. Fratini, M.G. Page, R. Giorgi, H. Cölfen, P. Baglioni, B. Demé, T. Zemb, Competitive
488 Surface Adsorption of Solvent Molecules and Compactness of Agglomeration in Calcium
489 Hydroxide Nanoparticles, *Langmuir*. 23 (2007) 2330–2338. doi:10.1021/la062023i.
- 490 [33] E. Hansen, E. Doehne, J. Fidler, J. Larson, B. Martin, M. Matteini, C. Rodriguez-Navarro, E.
491 Pardo, C. Price, A. de Tagle, J. Teutonico, N. Wiess, A review of selected inorganic
492 consolidants and protective treatments for porous calcareous materials, *Rev. Conserv.* 4 (2003)
493 13–25.
- 494 [34] C. Rodriguez-Navarro, A. Suzuki, E. Ruiz-Agudo, Alcohol Dispersions of Calcium Hydroxide
495 Nanoparticles for Stone Conservation, *Langmuir*. 29 (2013) 11457–11470.
496 doi:10.1021/la4017728.
- 497 [35] G. Wheeler, Alkoxysilanes and the Consolidation of Stone, Getty Conservation Institute, Los
498 Angeles, 2005.
- 499 [36] M.J. Mosquera, D.M. de los Santos, A. Montes, L. Valdez-Castro, New Nanomaterials for
500 Consolidating Stone, *Langmuir*. 24 (2008) 2772–2778. doi:10.1021/la703652y.
- 501 [37] G.W. Scherer, S.A. Pardenek, R.M. Swiatek, Viscoelasticity in silica gel, *J. Non. Cryst. Solids*.
502 107 (1988) 14–22. doi:https://doi.org/10.1016/0022-3093(88)90086-5.
- 503 [38] G.W. Scherer, Theory of Drying, *J. Am. Ceram. Soc.* 73 (1990) 3–14. doi:10.1111/j.1151-
504 2916.1990.tb05082.x.
- 505 [39] A. Zornoza-Indart, P. Lopez-Arce, Silica nanoparticles (SiO₂): Influence of relative humidity
506 in stone consolidation, *J. Cult. Herit.* 18 (2016) 258–270.
507 doi:https://doi.org/10.1016/j.culher.2015.06.002.
- 508 [40] C. Horie, *Materials for conservation : organic consolidants, adhesives, and coatings*, London ;
509 Boston; Butterworths, 1987.
- 510 [41] R. Feller, *On picture varnishes and their solvents*, Rev. and e, 1985.
- 511 [42] G. Amoroso, *Trattato di scienza della conservazione dei monumenti*, Firenze, 2002.
- 512 [43] O. Chiantore, M. Lazzari, Photo-oxidative stability of paraloid acrylic protective polymers,
513 *Polymer (Guildf)*. 42 (2001) 17–27. doi:https://doi.org/10.1016/S0032-3861(00)00327-X.

- 514 [44] E. Jablonski, T. Learner, J. Hayes, M. Golden, Conservation concerns for acrylic emulsion
515 paints, *Stud. Conserv.* 48 (2003) 3–12. doi:10.1179/sic.2003.48.Supplement-1.3.
- 516 [45] L. Lazzarini, *Pietre e marmi antichi. Natura, caratterizzazione, origine, storia d'uso, diffusione,*
517 *collezionismo*, Padova, 2004.
- 518 [46] N. Careddu, G. Marras, The effects of solar UV radiation on the gloss values of polished stone
519 surfaces, *Constr. Build. Mater.* 49 (2013) 828–834.
520 doi:<https://doi.org/10.1016/j.conbuildmat.2013.09.010>.
- 521 [47] D. Lerche, Dispersion Stability and Particle Characterization by Sedimentation Kinetics in a
522 Centrifugal Field, *J. Dispers. Sci. Technol.* 23 (2002) 699–709. doi:10.1081/DIS-120015373.
- 523 [48] ASTM International, ASTM D2244-16 - Standard Practice for Calculation of Color Tolerances
524 and Color Differences from Instrumentally Measured Color Coordinates, (2016).
- 525 [49] G. Wyszecki, W. Stiles, *Color Science: Concepts and Methods, Quantitative Data and*
526 *Formulae*, 2nd Edition, 2000, 2000.
- 527 [50] A. Brunelli, A. Zabeo, E. Semenzin, D. Hristozov, A. Marcomini, Extrapolated long-term
528 stability of titanium dioxide nanoparticles and multi-walled carbon nanotubes in artificial
529 freshwater, *J. Nanoparticle Res.* 18 (2016) 113. doi:10.1007/s11051-016-3412-3.
- 530 [51] M. Elliot, Morphology and life history of *Haematococcus pluvialis*, *Arch. Protistenk.* 82
531 (1934) 250–272.
- 532 [52] S. Boussiba, Carotenogenesis in the green alga *Haematococcus pluvialis*: Cellular physiology
533 and stress response, *Physiol. Plant.* 108 (2000) 111–117. doi:10.1034/j.1399-
534 3054.2000.108002111.x.
- 535 [53] G. Wypych, *Handbook of Material Weathering* 5th Edition, Elsevier, 2013.
- 536
537
538

Supporting Information

Consolidation of Vicenza, Arenaria and Istria stones: a comparison between nano-based products and acrylate derivatives

Giulia Gheno¹, Elena Badetti², Andrea Brunelli², Renzo Ganzerla¹, Antonio Marcomini^{2*}

¹DSMN - Department of Molecular Sciences and Nanosystems, Ca' Foscari University of Venice, Scientific Campus in Via Torino 155, 30172 Mestre (VE), Italy

²DAIS - Dept. of Environmental Sciences, Informatics and Statistics, Ca' Foscari University of Venice, Scientific Campus in Via Torino 155, 30172 Mestre (VE), Italy

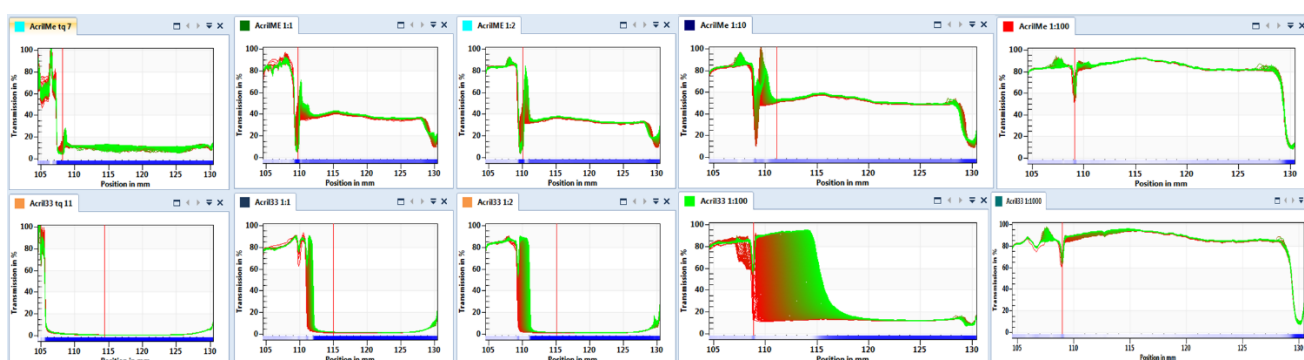


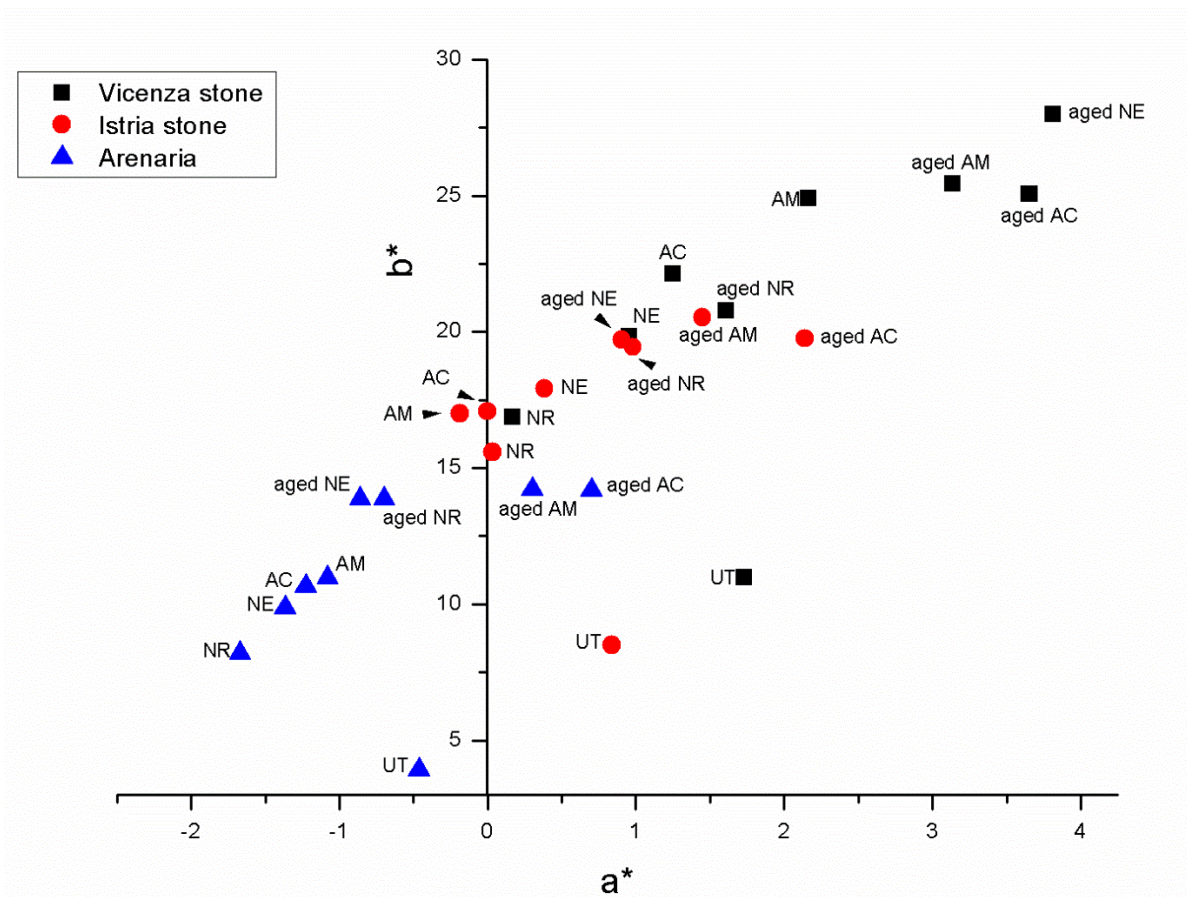
Figure S1 – Trasmission profiles of Acril Me fresh, 1:2, 1:4, 1:10 and 1:100 dilution with MilliQ water (top) and of Acril 33 fresh, 1:2, 1:4, 1:100 and 1:1000 dilution with MilliQ water (down).

Table S1. BET surface area and total pore volumes determined at P/P_0 of 0.98 for Vicenza stone, Arenaria and Istria stone.

Sample	BET surface area (m^2/g)	Total Pore volumes (cm^3/g)
Vicenza stone	$5.5 \cdot 10^{-2}$	$2.5 \cdot 10^{-3}$
Arenaria	4.3	$8.0 \cdot 10^{-3}$
Istria stone	$3.0 \cdot 10^{-2}$	n.d.

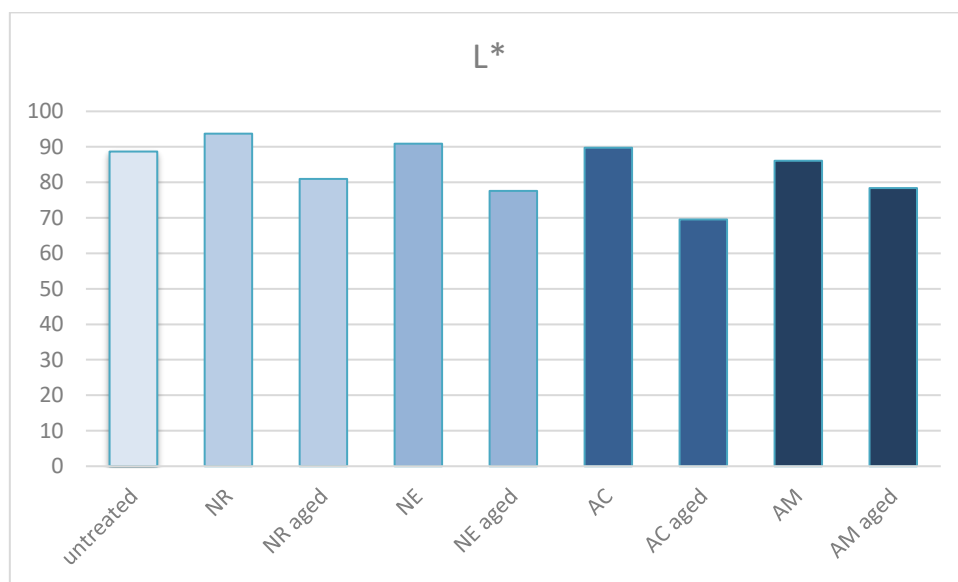
Table S2. Quantity (g) of absorbed product (NanoRestore, NanoEstel, Acril 33 and Acril ME) from the Vicenza stone, Arenaria and Istria stone.

Sample	Vicenza stone (g)	Arenaria (g)	Istria stone (g)
NanoRestore	0.031 ± 0.004	0.018 ± 0.003	0.006 ± 0.001
NanoEstel	0.800 ± 0.030	0.011 ± 0.020	0.010 ± 0.003
Acril 33	0.460 ± 0.040	0.170 ± 0.040	0.073 ± 0.007
Acril ME	0.630 ± 0.050	0.200 ± 0.040	0.150 ± 0.030



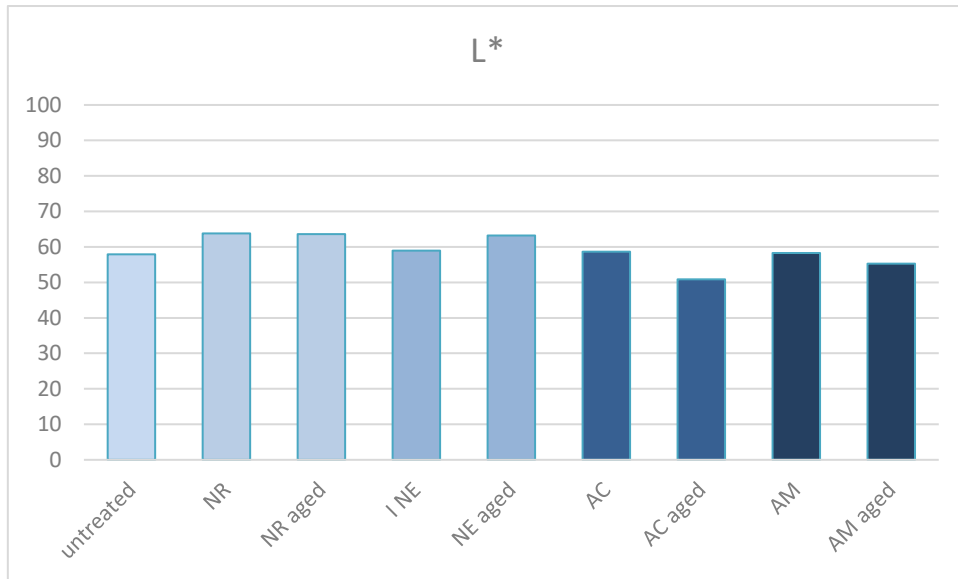
564
565
566
567
568
569

Figure S2- Plot of a^* versus b^* values determined for untreated (UT), fresh and aged at outdoor Venezia Mestre environments treated samples with NanoRestore (NR), NanoEstel (NE), Acril 33 (AC) and Acril ME (AM). a = Vicenza stone (V); b = Arenaria (A); c = Istria stone (I).



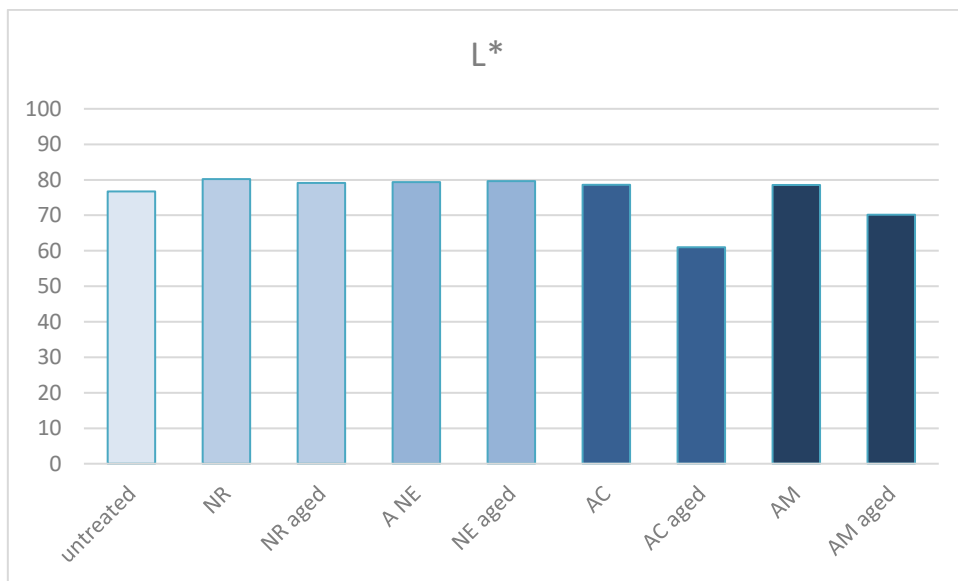
570
571
572
573

Figure S3- Plot of L^* values of untreated, fresh and aged (outdoor Venice-Mestre environment for two years) Vicenza stone with NanoRestore (NR), NanoEstel (NE), Acril 33 (AC) and Acril ME (AM).



574
575
576
577
578

Figure S4- Plot of L* values of untreated, fresh and aged (outdoor Venezia Mestre environment for two years) Arenaria with NanoRestore (NR), NanoEstel (NE), Acril 33 (AC) and Acril ME (AM).



579
580
581
582
583
584
585
586
587
588

Figure S5- Plot of L* values of untreated, fresh and aged (outdoor Venezia Mestre environment for two years) Istria stone with NanoRestore (NR), NanoEstel (NE), Acril 33 (AC) and Acril ME (AM).



589

590 Figure S6. Micrographs (20x) of the surface morphology of the stone samples treated with
 591 NanoRestore, NanoEstel, Acril 33 and Acril ME and exposed at Venezia Mestre outdoor condition
 592 for two years.

593

594

595

596

597

598

599

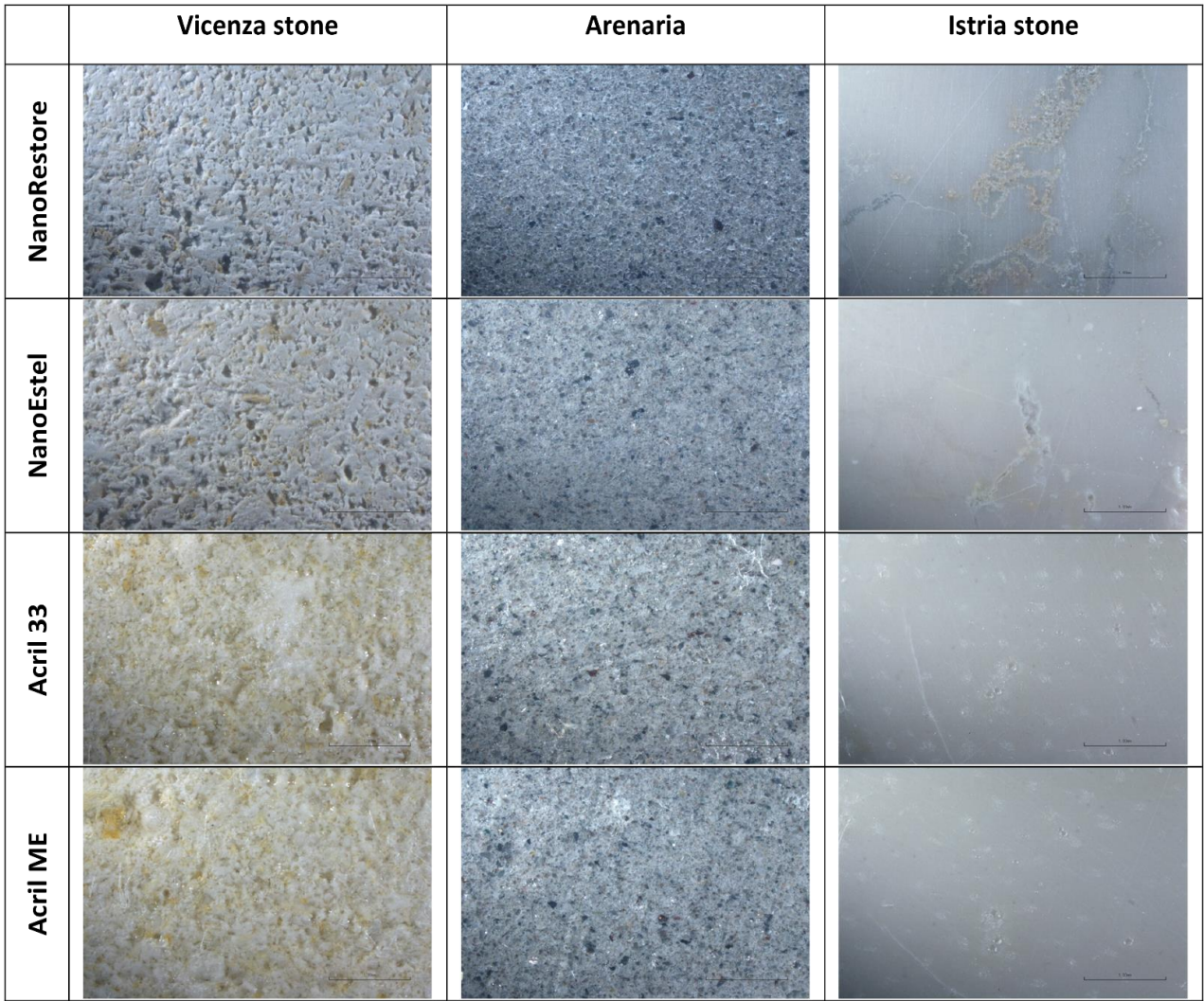
600

601

602

603

604



605

606

607

608

609

Figure S7. Micrographs (10x) of the surface morphology of the stone samples treated with NanoRestore, NanoEstel, Acril 33 and Acril ME and exposed at UVB aging for 1200 hours.